CHAPTER IV.

Self-assembling doxorubicin-tocopherol succinate prodrug as a new drug delivery system: synthesis, characterization and in vitro anticancer activity

Self-assembling doxorubicin-tocopherol succinate prodrug as a new drug delivery system: synthesis, characterization and in vitro anticancer activity

Nicolas Duhem, Vincent Pourcelle, Jean-Marc Schumers, Olivier Bertrand, Cécile S. LeDuff, Stephanie Hoeppener, Ulrich S. Schubert, Jean-François Gohy, Jacqueline Marchand-Brynaert, Véronique Préat

ABSTRACT

Self-assembled prodrugs forming nanoaggregates are a promising approach to enhance the antitumor efficacy and to reduce the toxicity of anticancer drugs. To achieve this goal, doxorubicin was chemically conjugated to D-α-tocopherol succinate through an amide bond to form N-doxorubicin-α-D-tocopherol succinate (N-DOX-TOS). The prodrug self-assembled in water into 250 nm nanostructures when stabilized with D-α-tocopherol polyethylene glycol 2000 succinate. Cryo-TEM analysis revealed the formation of nanoparticles with a highly ordered lamellar inner structure. NMR spectra of the N-DOX-TOS nanoparticles indicated that N-DOX-TOS is located in the core of the nanoparticles while PEG chains and part of the tocopherol are in the corona. High drug loading (34% w/w) and low in vitro drug release were achieved. In vitro biological assessment showed significant anticancer activity and cellular uptake of N-DOX-TOS nanoparticles. N-DOX-TOS nanoparticles might have the potential to improve DOX-based chemotherapy.

KEYWORDS

Cancer, Nanoparticle, Prodrug, Self-assembly, Tocopherol, Doxorubicin

I. INTRODUCTION

Doxorubicin (DOX) is a highly effective and widely used chemotherapeutic agent against various types of cancers including breast cancers, urothelial cancers, hematopoietic malignancies and other solid tumors (*1*). DOX causes DNA damages and induction of apoptosis through the inhibition of topoisomerase II and stabilization of ternary drug-topoisomerase II-DNA complex (*2*). Its effectiveness is limited by its short half-life in the bloodstream and its cytotoxicity in normal tissues. The cumulative dose of DOX is limited to 500-600 mg/m² to avoid cardiotoxicity, while it should be increased for tumor treatment (*1, 3, 4*). Therefore, there is a need to find out an efficient way to deliver DOX in attempt to increase its activity and to limit its toxicity.

Utilization of nanomedicines in oncology has attracted the attention of many research endeavors in recent years. Nanomedicines provide better biopharmaceutical properties to anticancer drugs. They can decrease their toxicity and side effects, improve their bioavailability and stability and prolong their circulation time (*1, 5-7*). Moreover, nanomedicines can passively accumulate in tumor through the enhanced permeation and retention (EPR) effect (*8*).

One major limitation of most of the nanocarriers is the low drug loading efficiency *i.e.* low weight ratio of drug/nanocarrier. Hence, amphiphilic prodrugs that self-assemble and form nanostructures have been designed (*9*). Prodrugs when administered must be chemically or enzymatically degraded *in vivo* to the parent active drug, preferably in a controlled or predictable manner (*5*). Lipid-drug conjugates and polymer-drug conjugates have extensively been investigated as prodrugs for cancer treatment and have shown promising results in preclinical and some clinical studies (*9-11*). Self-assembled prodrug-based delivery concept can be an answer to common prodrug limitations. Harnessing the advantages of prodrug and nanomedicine strategies in cancer therapy can lead to strongly efficient therapeutic options to achieve (i) maximum drug loading efficiency, (ii) controlled and prolonged release kinetics and (iii) passive targeting to the tumor. In particular, the lipid squalene has been chemically conjugated with various therapeutic molecules to construct nanoassemblies of 100-300 nm that are promising for cancer treatment (*12-14*).

In this paper, we applied the self-assembled prodrug-based delivery concept to DOX. We have developed a vitamin E derivative of doxorubicin, N-doxorubicin-α-D-tocopherol succinate (N-DOX-TOS). Vitamin E derivatives are particularly promising for the formation of anticancer drug conjugates. Beside the nontoxic and biocompatible characteristics of the vitamin E family, the synergic ability of D-α-Tocopherol succinate (TOS) to act with a chemotherapeutic drug, improving tumor response to chemotherapy, has been demonstrated (*15*). TOS has been found to inhibit the proliferation of various cancer cells *in vitro* and *in vivo*. Cells that can respond to antitumor effects mediated by TOS include inter alia human neuroblastoma cells, prostate carcinoma cells, promyelotic cells, gastric cancer cells and breast cancer cells (*15-18*). Previous experiment in our lab have shown that when TOS is grafted on glucosamine, the derivative spontaneously self-assembled in water in the presence of D-α-tocopheryl polyethylene glycol 1000 succinate (TPGS) acting as a stabilizer, by using a simple nanoprecipitation method (unpublished data).

The aim of this study was to develop N-DOX-TOS nanoparticles in order to increase the anticancer effect and/or to decrease the side effects of the parent drug. An amido prodrug (N-DOX-TOS) was synthesized and the effectiveness of the TOS conjugation on the drug was determined by ^{1}H-RMN, ^{13}C-RMN, mass spectrometry and HPLC. The physico-chemical characteristics of N-DOX-TOS formulated as nanoparticles such as size and morphology of the supramolecular structures were explored. Finally, the *in vitro* cytotoxicity and the cellular uptake of the N-DOX-TOS nanoparticles were determined by using MCF-7 breast cancer cell line.

II. EXPERIMENTAL

II.1. MATERIALS

All solvents, including anhydrous solvents, and reagents were purchased from Acros Organics, Alfa Aesar, Fluka, Sigma-Aldrich or VWR, and used without any further purification. Deuterated solvents were purchased from Euriso-top (France). Doxorubicin hydrochloride (DOX, USP31 standard) was purchased from Chemieliva Pharmaceutical (China). Cytarabine (≥90%) D-(+)-Glucosamine hydrochloride (≥99%) and α-Tocopherol succinate (TOS) were purchased from Sigma. All other reagents were purchased from Acros Organics, Fluka and Sigma-Aldrich. All reactions under dry conditions were performed under argon atmosphere in flame-dried glassware. Poly(ethylenoxide) monomethylether (PEO45-OH) (Mn=2000 g/mol) was dried by azeotropic cycles with toluene prior to use. Dichloromethane (DCM) was distilled over CaH_2 and TOS was dried 24 h in a vacuum oven at 35°C prior to use.

II.2. INSTRUMENTATION

^{1}H (500 MHz) and ^{13}C (125 MHz) NMR spectra were recorded on a Bruker Avance 500 spectrometer. Spectra were obtained in $CDCl_3$, $(CD_3)_2SO$ or D_2O at room temperature. Chemical shifts δ are reported in ppm and are calibrated on the solvent residual signal at 7.26 and 77.16 for $CDCl_3$ and at 2.50 and 39.52 for $(CD_3)_2SO$. For NMR spectra acquired in D_2O, trimethyl silyl-3-propionic acid-d4-sodium salt was used as reference (0 ppm). NMR coupling constants (J) are reported in hertz. High Resolution Mass Spectrometry (HRMS) analyses were performed using a QExactive equipment (Thermo Scientific). TLC analysis was performed on Merck silica gel 60 F_{254} with detection under UV light, and flash chromatography was performed on silica gel (40-60 mesh) purchased from Rocc (Belgium). The HPLC system consisted of a Waters (Waters, USA) Alliance 2699 separation module combined with a Waters 2998 photodiode array detector, a Waters 600 pump, a Waters 717 autosampler and Waters 486 absorbance detector. Analytical separations were performed with a Waters XBridge C18 column (4.6x50 mm, 2.5µm) equipped with a conventional pre-column. HPLC analyses were performed at a temperature of 25°C with a volume of full-loop injections of 5 µL. The flow rate was 1 mL/min. Detection was performed at 254/280 nm and

online UV/Vis absorbance scans were performed. For N-DOX-TOS a MeOH:H_2O gradient was applied (from 1:1 to 1:0).

II.3. SYNTHESIS OF N-D-A-TOCOPHEROL SUCCINATE DERIVATIVE OF DOXORUBICIN

The N-D-α-Tocopherol succinate derivative of doxorubicin (N-DOX-TOS) was synthesized by covalent coupling of DOX with TOS onto the amino group of the glucosamine (Figure 1). DOX.HCl (251 mg, 0.43 mmol, 1.20 equiv.) was dissolved in warm DMF (5 mL) prior to the addition of N-methyl morpholine (51 mg, 0.50 mmol, 1.4 equiv.), hydroxybenzotriazole (HOBt) (68 mg, 1.50 mmol, 1.4 equiv.) and TOS (191. mg, 0.36 mmol, 1 equiv.). Then, (1-ethyl-3(3-dimethylaminopropyl)carbodiimide hydrochloride (EDC.HCl) (98 mg, 0.50 mmol, 1.4 equiv.) dissolved in DCM (15 mL) was added drop-wise to the reaction mixture under stirring and the solution was heated at 55°C for 24h. 20 mL of DCM were then added and the reaction mixture was washed four times with 60 mL of brine. Then the organic layer was dried on $MgSO_4$, filtered, evaporated and dried under vacuum for 24h. The resulting red powder (yield 336 mg, 88%, HPLC purity ≥ 98%) was collected and used without further with TOS (see Supporting Information S1).

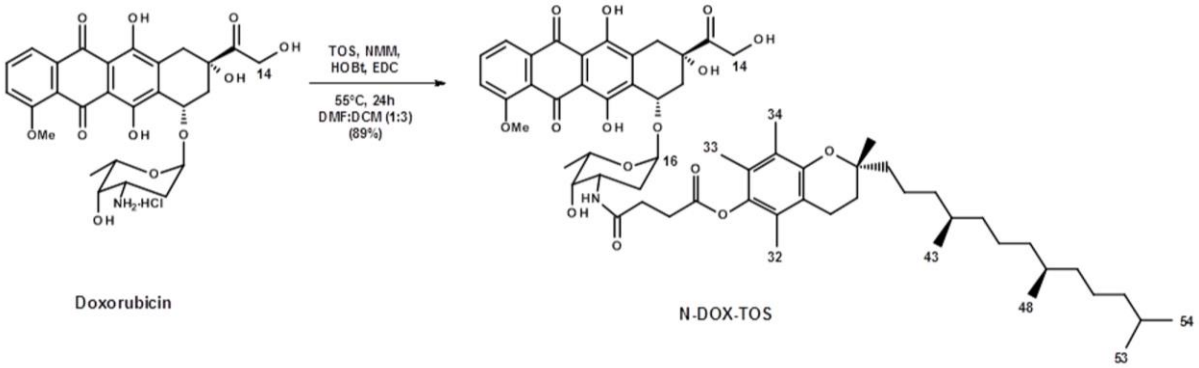

Figure 1. Synthesis of N-DOX-TOS.

^{1}H NMR (500 MHz, $CDCl_3$): δ 0.83 (m, 6H), 0.86 (d, 6H, J = 7Hz), 1.05-1.13 (m, 6H), 1.2 (s, 3H), 1.24 (m, 10H), 1.27 (d, 3H, J = 6Hz), 1.36 (m, 3H), 1.51 (m, 2H), 1.72 (m, 2H), 1.8 (m, 2H), 1.91 (s, 3H), 1.95 (s, 3H), 2.04 (s, 3H), 2.15 (dd, 1H, J = 14Hz. J = 4Hz), 2.24 (bs, 1H), 2.32 (d, 1H, J = 15Hz), 2.53 (m, 4H), 2.88 (m, 1H), 2.96 (d, 1H, J = 18Hz), 2.96 (bs, 1H), 3.03 (bs, 1H), 3.24 (d, 1H, J = 18Hz), 3.64 (s, 1H), 4.05 (s, 3H), 4.11 (m, 1H), 4.12 (m, 1H), 4.76 (s, 2H), 5.25 (m, 1H),

5.48 (m, 1H), 5.99 (d, 1H, J = 8.3Hz), 7.37 (d, 1H, J = 8.2Hz), 7.76 (dd, 1H, J = 8.1Hz), 8 (d, 1H, J = 8.1Hz).^{13}C NMR (125 MHz, $CDCl_3$): δ 11.9, 12.3, 13.1, 17, 19.8, 19.9, 20.7, 21.1, 22.8, 22.9, 24, 24.6, 24.9, 28.1, 29.3, 29.8, 31.2, 32.8, 32.9, 34.1, 35.8, 37.4, 37.6, 39.5, 40.2, 45.6, 56.8, 65.7, 67.3, 69.2, 69.8, 75.2, 76.7, 100.9, 111.5, 111.7, 117.5, 118.5, 119.9, 120.9, 123.1, 125, 126.7, 133.7, 135.6, 135.9, 140.5, 149.5, 155.7, 156.3, 161.1, 170.8, 171.9, 186.7, 187.1, 214; HRMS-ESI (m/z): $[M+Na]^+$ calculated for $C_{60}H_{81}NO_{15}Na$: 1078.54984 found : 1078.54992.

II.4. SYNTHESIS OF D-A-TOCOPHEROL POLYETHYLENE 2000 SUCCINATE

Under argon, a solution of dicyclocarbodiimide (DCC) (189 mg, 0.92 mmol, 1.2 equiv.) in dry DCM (5 mL) was added drop-wise, at 0 °C to a stirred mixture of PEO_{45}-OH (1425 mg, 0.76 mmol, 1.0 equiv.), 4-dimethylaminopyridine DMAP (11 mg, 0.08 mmol, 0.1 equiv.) and TOS (485 mg, 0.92 mmol, 1.2 equiv.) in dry DCM (14 mL). The mixture was then slowly warmed to 20 °C. A white precipitate corresponding to the N,N'-dicyclohexyl urea appeared after 20 minutes of reaction time. The reaction medium was - stirred at 20 °C for 18 h. The mixture was filtered in order to remove the precipitate and the mixture was washed twice with 0.05 M HCl and twice with saturated $NaHCO_3$ solutions (*19*). The organic phase was dried over Na_2SO_4, filtered and the solvent was removed in vacuo. The residue was dissolved in a minimum of THF and precipitated twice in a diethyl ether/hexane (1:1, v/v) mixture affording a white powder which was further dried in vacuo at 35 °C for 24 h (yield : 1775 mg, 92 %).

^{1}H NMR (500 MHz, $CDCl_3$): δ (t, 2H, ^3J =4.5 Hz, CH_2), 3.64 (brs, 178H, CH_2), 3.37 (s, 3H, CH_3), 2.92 (t, 2H, ^3J =6.5 Hz, CH_2), 2.79 (t, 2H, ^3J =6.5 Hz, CH_2), 2.57 (t, 2H, ^3J =6.5 Hz, CH_2), 2.07 (s, 3H, CH_3), 2.00 (s, 3H, CH_3), 1.96 (s, 3H, CH_3), 1.90-1.65 (m, 2H, CH_2), 1.60-1.00 (m, 24H, CH, CH_2, CH_3), 0.86 (d, 6H, ^3J =6.5 Hz, CH_3), 0.84 (d, 6H, ^3J =6.5 Hz, CH_3).

II.5. PREPARATION OF DOX-TOS NANOPARTICLES

The preparation of N-DOX-TOS nanoparticles was performed by using the nanoprecipitation technique (*20*). Briefly, a solution of N-DOX-TOS and $TPGS_{2000}$ (2:1 w/w) in acetone was added dropwise under stirring (500 rpm) into 2.5 mL of 5% aqueous glucose solution. Precipitation of the nanoassemblies occurred spontaneously. Acetone was completely

evaporated using a Rotavapor® to obtain a free suspension of N-DOX-TOS nanoparticles in water (4 mg/mL).

II.6. PHYSICO-CHEMICAL CHARACTERISTICS OF THE NANOPARTICLES

The average N-DOX-TOS nanoparticle size and ζ potential were determined, respectively, by photon correlation spectroscopy and laser Doppler velocimetry, combined with phase analysis light scattering (PALS) using a Zetasizer® Nano ZS (Malvern Instruments, UK). The instrument was calibrated with reference polystyrene nanoparticles (Malvern Instruments, UK). The particle size was also assessed after storage at 4 ° C for 6 months. All assays were performed in triplicate.

The loading efficiency (LE) was determined as the amount of DOX equivalents in the N-DOX-TOS nanoparticles.

$$LE = \frac{Amount\ of\ DOX\ equivalents\ in\ nanoparticles}{Amount\ of\ prodrug + Amount\ of\ TPGS2000}$$

Cryogenic transmission electron microscopy (Cryo-TEM) investigations were conducted on a Philips CM-120. Samples were vitrified in a home-built blotting device in liquid ethane. Samples were transferred in a liquid nitrogen environment into a Gatan 626 holder at temperatures lower than -180 °C and were imaged at low electron doses. The diameter of the observed nanoparticles and the period of the lamellar internal structures were calculated from cryo-TEM pictures by averaging measurements performed on more than 100 objects recorded from different areas on the cryo-TEM grid.

II.7. NMR OF NANOPARTICLES IN WATER

N-DOX-TOS nanoparticles were prepared as described above but using deuterated solvents (*i.e.* $(CD_3)_2CO$ and D_2O). The final concentration of the system was 4 mg of N-DOX-TOS and 2 mg of $TPGS_{2000}$ in 1 mL of D_2O. The ^{1}H-NMR (500 MHz) spectra were acquired at 20 °C with the following experimental settings : delay between scans (D1) of 10 s, 5000 scans (16h), acquisition time 1.5 s, number of points 24576, spectral window 16 ppm. The HDO signal was suppressed using pre-saturation prior to measuring the ^{1}H spectrum.

II.8. NANOPARTICLE STABILITY

To determine the stability of the nanoparticles, 1 mL of N-DOX-TOS nanoparticles made of 1mg of the prodrug N-DOX-TOS and 0.5 mg of $TPGS_{2000}$ was placed in a 1 mL dialysis bag (molecular mass cut-off 1kDa, Spectra/Por®, Spectrum Laboratory Inc., Canada). The dialysis bag was incubated with gentle stirring in 30 mL of PBS (pH 7.4) which was changed at predetermined time points. The collected dialysate was analyzed by fluorescence (Perkin-Elmer LS-30, Perkin-Elmer Ltd, Beaconsfield, UK, λex = 475 nm, λem = 590 nm). A DOX calibration curve was established (0.04 μg/mL -1 μg/mL). All assays were performed in triplicate.

II.9. CELL EXPERIMENTS

II.9.1. Cell lines

MCF-7 breast adenocarcinoma cells (American Type Culture Collection, ATCC® HTB-22™) were employed as in vitro models for the assessment of DOX and N-DOX-TOS nanoparticles. The cells were cultured in DMEM medium supplemented with 10% FBS, 1% penicillin–streptomycin solution, 1% pyruvate, 1% glucose (Invitrogen Life technologies, Merelbeke, Belgium) .

II.9.2. In vitro anticancer activity of DOX-TOS nanoparticles

Cytotoxicity of N-DOX-TOS nanoparticles was evaluated in MCF7 cells and was compared with that of DOX. Cells were seeded at a density of 8 to 12 x 10^4 cells/well, depending of the drug incubation time, in 96-well transparent plates and incubated for 24 h. The medium was then replaced by the free DOX or N-DOX-TOS nanoparticles at various drug concentrations. The incubation was carried out for 24, 48 and 72h. The cell viability was determined by the 1-(4,5-dimethylthiazol-2-yl)-3,5-diphenylformazan (MTT, Sigma) assay. At 24, 48, 72 h, the medium was removed. MTT (0.5 mg/mL) in medium was added and the cells were incubated for 3h. The media was removed from all wells and 100 μL of DMSO (Merck, Germany) were added to dissolve the formazan by-product. Absorbance of the 96-well plates was assessed with a Multiscan EX (Thermo Fisher Scientific Corporation, USA) at 620 nm. From the absorbance, the viability of the cells expressed in percentages was calculated using the

negative control as reference (100% of viability). Triton (1%) was used as positive control. All assays were performed in triplicate (N = 3, n = 4). IC_{50} were calculated by using a nonlinear regression (log(inhibitor) versus response, variable slope) using Graphpad prism 5 for windows.

II.9.3. Cellular uptake by fluorescence microscopy

MCF7 cells were cultured in 12-well plates containing a small glass plate pre-coated with 100µl polylysine at a density of 2 x 10^5 cells/mL. One day after plating, MCF-7 cells were incubated with N-DOX-TOS nanoparticles or free DOX at 10 µM DOX-equivalent concentration at 37°C for 24 h. After incubation, medium was removed. Cells were fixed with 4% paraformaldehyde in PBS then washed 3 times with PBS. Cells were incubated 5 min with DAPI (0.1µg/mL diluted 10^4x in PBS) and washed three times with PBS. Cells were incubated 1h with Concanavalin A Alexa Fluor® 488 Conjugate (ConA) (1/200 in PBS, v/v) and then washed three times with PBS. Finally cells were mounted on Vectashield (Vector Lab Inc., USA) and examined with a fluorescence microscope (Axio Imager 2, Zeiss) using the 350 nm (DAPI, blue), 488nm (ConA, green) and 595 nm (DOX, red) filters, and photographed with an AxioCam MRc5 camera (Zeiss, Germany).

II.10. STATISTICS

Statistical analyses were completed using Graphpad prism 5 for windows. IC_{50} values were compared with a 2-way ANOVA with a Bonferroni post-test.

III. RESULTS

III.1. SYNTHESIS AND CHARACTERIZATION OF THE N-DOX-TOS

As shown on Fig. 1, the prodrug of DOX based on tocopherol conjugation, namely N-doxorubicin-D-α-tocopherol succinate (N-DOX-TOS), was synthesized using a classical carbodiimide coupling method to bind the carboxylic acid of TOS to the amino group of DOX. The amido derivative of DOX was developed as amido link is easier to handle then other common derivatives of DOX using hydrazine or ester links. This synthesis was first optimized for the coupling of cytarabine with TOS to obtain the corresponding cytarabine-TOS conjugate. This prodrug did not demonstrate self-assembling property and consequently was not employed in this study (see Supporting Information S1). An excess of DOX was used to drive the coupling reaction to completion and to allow simple purification by successive washings with brine. This strategy demonstrated to be successful since the N-DOX-TOS prodrug was obtained in high purity (≥98% from HPLC). The exclusive linkage of TOS onto the amine group of DOX was unambiguously established by proton and carbon NMR (1D and 2D experiments, *i.e.* HMBC and HMQC).

We similarly synthesized $TPGS_{2000}$ by linking tocopherol succinate to PEG of a molar mass of 2,000 g/mol via an ester bond as described elsewhere (*21*).

III.2. FORMULATION OF DOX-TOS NANOPARTICLES

The TOS derivative of DOX was designed to form anticancer nanoparticles with (i) high drug loading (>30%) (ii) self-assembling properties and easy manufacture (iii) size adapted to intravenous injection and to the EPR effect to passively target DOX in the tumor (*8, 22*).

N-DOX-TOS alone was able to self-assemble in water, but the nanoparticles tended to form large aggregates. Hence, a PEGylated vitamin E derivative, $TPGS_{2000}$, was added as a stabilizer to their formulation. PEGylation is known to stabilize nanoparticles by steric hindrance (21). $TPGS_{2000}$ was chosen because it has been previously demonstrated that $TPGS_{2000}$-based micelles were more stable than the $TPGS_{1000}$ ones bearing shorter PEG chains (*21*). Longer PEG chains are helpful to avoid elimination via the reticuloendothelial system by reducing the protein interactions on the surface, thus preventing opsonin binding, extending blood

circulation times and reducing liver accumulation (*23, 24*). Finally, PEG bearing targeting units such as folate, antibodies or peptides, can be introduced in order to have targeted drug delivery systems (*21*).

However, pegylated vitamin E did not improve sufficiently the size and the stability of cytarabine-TOS prodrug we first synthesized. Cytarabine-TOS prodrug formed micronic aggregates without stabilizer. In presence of pegylated vitamin E, cytarabine-TOS prodrug formed submicronic nanoparticles but with large size and poly dispersity (800 nm, PDI: 0.4) (data not shown). Thus we decided to no longer study cytarabine-TOS prodrug as its features were not compatible with IV administration and EPR effect. These data highlights how important are the physico-chemical properties of the drug for the self-assembled ability of the prodrug. Cytarabine is a highly hydrophilic drug but DOX has an amphiphilic nature and is able to form oligomers in water. Oligomerization of DOX is due to the stacking of the planar aromatic rings of the anthracycline thanks to interaction between the π electrons of the planar rings (*25*). *The ability of DOX to oligomerize could play key role in the self-assembly properties of N-DOX-TOS and in the structure of the N-DOX-TOS nanoparticle described in the next section.*

The nanoparticles were obtained by using a simple nanoprecipitation method which consists in adding an acetone solution of N-DOX-TOS and $TPGS_{2000}$ drop-wise in water under stirring, and then to evaporate acetone under vacuum. $TPGS_{2000}$ was mandatory to stabilize the molecular structuration of the nanoparticles. TPGS might act as a stabilizer due to its amphiphilic character : a hydrophilic PEG chain and a hydrophobic tocopherol head anchored in the lipidic part of the nanoparticle (*26*).

In contrast to DOX solution, the dispersion looked as an opaque, milky red solution (see Supporting Information S2). The best ratio of N-DOX-TOS/$TPGS_{2000}$ was 2:1 with a maximum concentration of 4 mg/mL of the prodrug to ensure the stability of the solution. At this concentration, corresponding to a DOX concentration of approximately 2 mg/mL, the N-DOX-TOS nanoparticles are in the concentration range of Doxil®, a commercially available liposomal formulation of DOX (*27*).

The amount of DOX loaded in the N-DOX-TOS nanoparticles was 34 wt %. This is one of the highest loading efficiency reported for DOX delivery systems. For instance, recently a DOX-

TPGS prodrug was synthesized with a drug loading of 26 wt % (*19*). Another example with a star-shape copolymer of lysine-linked di-$TPGS_{2000}$ (PLV2K) self-assembled in nano-structures of 16 nm was characterized by a 9.5 wt % drug loading (*28*). Our N-DOX-TOS nanoparticle drug loading is also 1 to 7 times higher than that of PLGA nanoparticles loaded or conjugated with DOX (*29-31*).Compared to nanomagnetite/squalenoyl-doxorubicin, a theragnostic system composed of DOX prodrug, the N-DOX-TOS nanoparticle payload was 47% higher(*23*).

III.3. PHYSICO-CHEMICAL CHARACTERISTICS OF THE DOX-TOS NANOPARTICLES

The hydrodynamic diameter of the nanoparticles estimated by DLS, was 234 nm for a 4 mg/mL prodrug concentration solution. The polydispersity in size was narrow (see Table 1). The ζ potential of the nanoparticles was −4.1 ± 0.7 mV. Since DOX-TOS nanoparticles do have phenol and carboxylic acid functions, one can assume that at neutral pH, part of the carboxylic acid groups is ionized and that (part of) the resulting carboxylate anions have a tendency to localize at the surface of the nanoparticles. This should lead to a slightly negative zeta potential as observed experimentally. These results suggest that N-DOX-TOS nanoparticles meet size and surface characteristics necessary to develop an injectable anticancer nanomedicine. To reach tumor site effectively, nanoparticle size should be much less than 400 nm (morelikely 150-200 nm) to diffuse through the tumor interstitium and the particle size higher than 10 nm to evade efficiently the renal elimination (*22*).

Table 1. Size analysis of DOX-TOS nanoparticles (N=3).

	Z-average diameter (nm)	PDI
Freshly synthesized nanoparticles	234 ± 12	0.101 ± 0.035
Nanoparticle stability after 6 months (4°C)	245 ± 8	0.074 ± 0.027

The N-DOX-TOS nanoparticles were analyzed using cryo-TEM. Rather monodisperse nanoparticles with a diameter of 250±30 nm were observed throughout the whole sample (Fig. 2a). The characteristic size of these nanoparticles is in perfect in agreement with the hydrodynamic diameter measured by DLS. Other morphologies including rugby ball and

donut-like nanoparticles were occasionally observed (Fig. 2b and 2c), again with average sizes around 250 nm. All these morphologies display an internal lamellar substructure with a characteristic period of 5.5±0.5 nm visualized as alternating dark and clear bands in the cryo-TEM pictures. This points out towards a hierarchical self-assembly process in the investigated N-DOX-TOS nanoparticles. Particles with a nano-structured internal organization have been previously described for the so-called cubosomes. Cubosomes are dispersed particles of bicontinuous cubic liquid crystalline phase particles which are physically stable in an excess of water (*32*). From the examination of a large number of the nanostructured objects formed by N-DOX-TOS, it however appears that the internal structure of our nanoparticles is not compatible with the cubic structure of cubosomes but is rather characteristic of a lamellar organization (Fig. 2). Basically, surfactant molecules are known to self-organize into three types of organization: spheres, cylinders and lamellae. The type of structure that a given surfactant molecules will adopt has been rationalized by the so-called packing parameter introduced by Israelachvili (*33*). The packing parameter describes the optimum packing shape or curvature of a surfactant molecule as a function of its molecular structure. In the case of the investigated N-DOX-TOS molecule, one can assume that the value of the packing parameter is close to 1 and thus in favor of a lamellar organization. The alternating dark and clear lamellae observed in Fig. 2. should contain on one hand the DOX aromatic part and on the other hand the aliphatic part of TOS. The added stabilizing TGPS molecule should be rejected towards the surface of the nanoparticle to act as stabilizer. NMR studies reported below confirm this hypothesis. To the best of our knowledge no nanoparticles with an internal lamellar structure were reported so far from tocopherol derivatives. It should be noted that different types of internal nano-structurations have been observed for nanoparticles formed by squalenoyl-drug conjugates depending of their chemical structure. For example, gemcitabine-squalene was shown to self-assemble in inverse hexagonal phases resulting from the packing of cylinders of water-swollen gemcitabine molecules surrounded by the hydrophobic squalene moieties. Differently, 2'-3'-dideoxycytidine-squalen was shown to self-assemble in cubosomes (*13, 34, 35*).

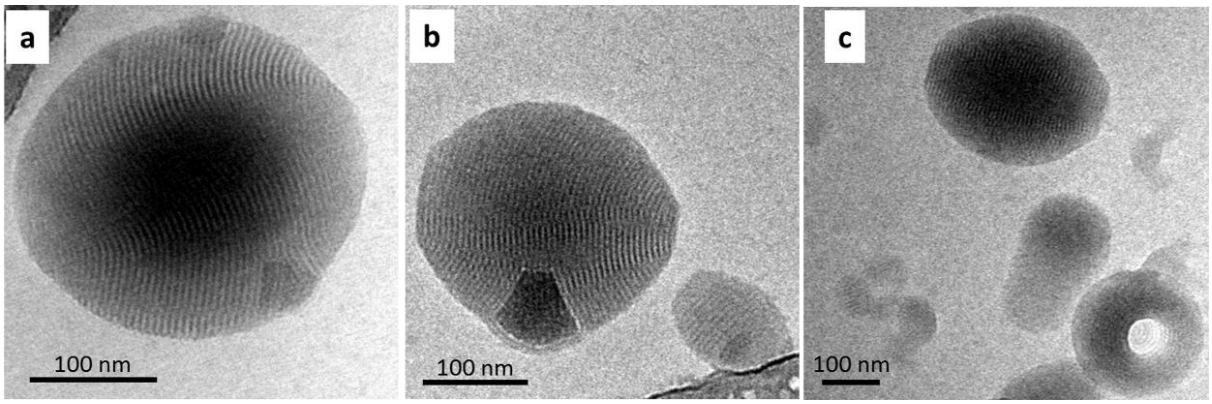

Figure 2. Cryo-TEM of N-DOX-TOS nanoparticles showing spherical nanoparticles as 2a, a rugby ball shaped nanoparticle as 2b and a donut as 2c.

In order to get a deeper insight in the structure of the N-DOX-TOS nanoparticles, ^{1}H NMR experiments were performed in D_2O (See Supporting Information S3). The measured spectrum shows predominance of PEG and tocopherol protons (Fig 3C). The protons of DOX are not visible on the NMR spectrum (Fig. 3), indicating that there are no free DOX molecules in the solution but rather that these are located inside the core of the nanoparticles into a collapsed solid state. This suggests an organization of the particles with N-DOX-TOS in the core of the structures where water cannot enter. The external shell of nanoparticles, *i.e.* the part exposed to water, is mostly constituted of PEG and part of the tocopherol linked to it. This is reinforced by the fact that we observe a broadening of tocopherol peaks (comparison between Fig 4A and Fig 4C). Moreover the integration of the peaks of the aliphatic methyl protons of TOS corresponds only to a small portion of the expected amount. For instance, considering the whole content in TOS, coming from TPGS and N-DOX-TOS contributions, the theoretical ratio of PEG integrals (at 3.71 ppm) to tocopherol methyl protons integrals (at 0.89 ppm) should be of 2.6. Taking into account the integrals of these peaks, we found an experimental ratio of 18.5. This result is close to the ratio calculated for the TOS in a TPGS molecule alone which is of 15.2 (for details see Supporting Information S4).

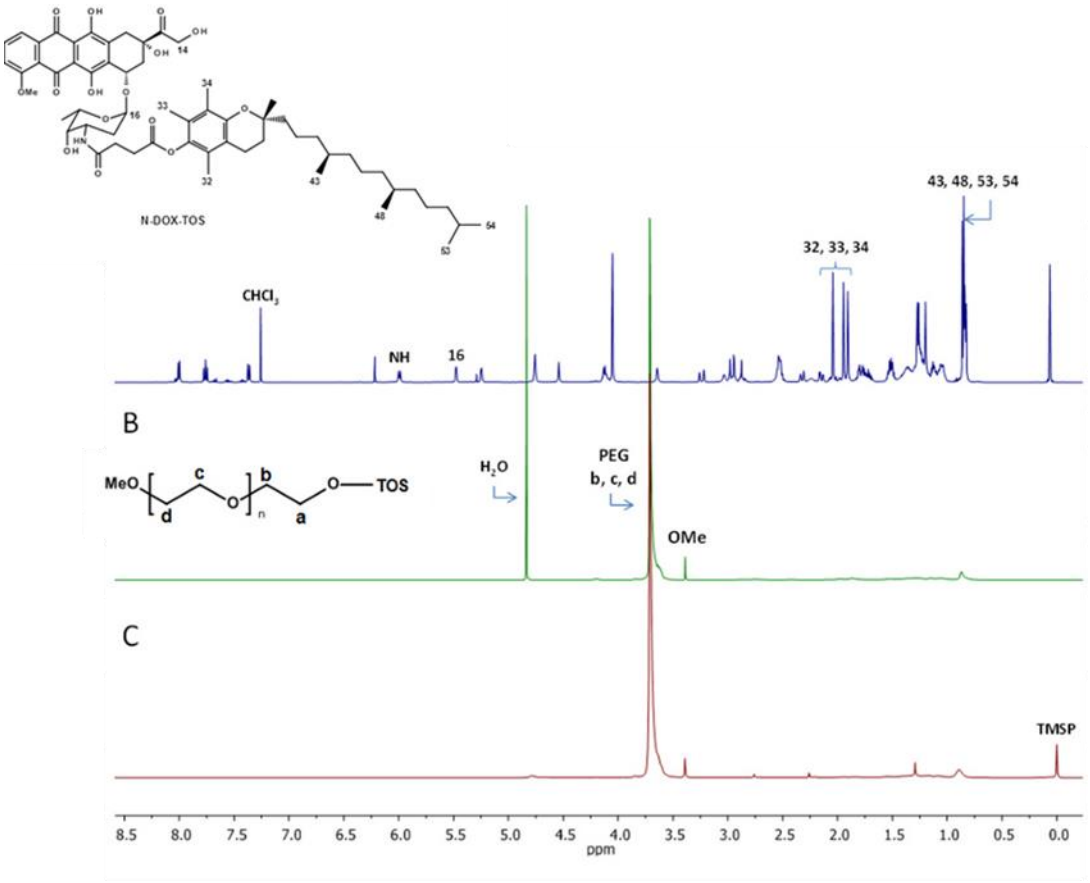

Figure 3. Stacked ^{1}H NMR full spectra of A) N-DOX-TOS in $CDCl_3$, B) TPGS in D_2O and C) nanoparticles containing N-DOX-TOS and TPGS in D_2O with presaturation of H_2O protons.

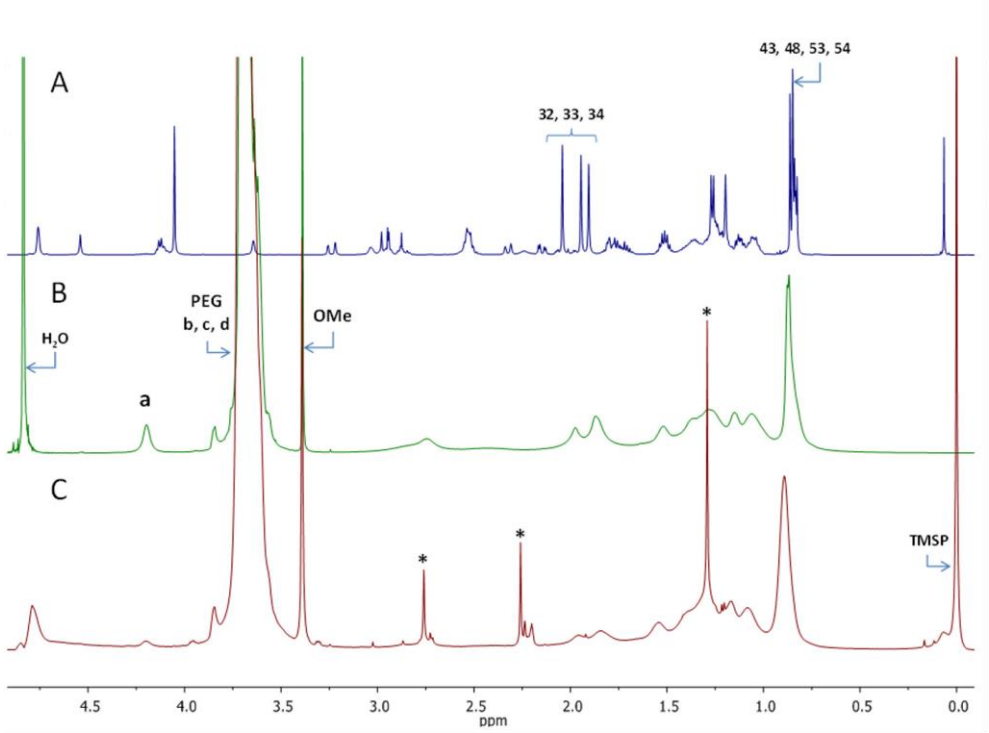

Figure 4. Stacked ^{1}H NMR spectra zoomed on the 0-4.75 ppm section, A) N-DOX-TOS in $CDCl_3$, B) TPGS in D_2O and C) nanoparticles containing N-DOX-TOS and TPGS in D_2O with presaturation of H_2O protons ("*"indicates unidentified impurities removed by dialysis).

Based on the cryo-TEM and NMR spectra collected on the nanoparticles, we suggest the nanoparticle structure illustrated in Fig. 5, where the N-DOX-TOS is located in the core of the nanoparticles with a segregation between DOX and TOS domains giving rise to the alternating lamellae as observed by cryo-TEM, and the TPGS segments pointed out towards the solution to act as stabilizers. Finally, it should be highlighted that the internal lamellar organization in N-DOX-TOS is different from previously reported cubic and hexagonal packing of cylinders for other systems.

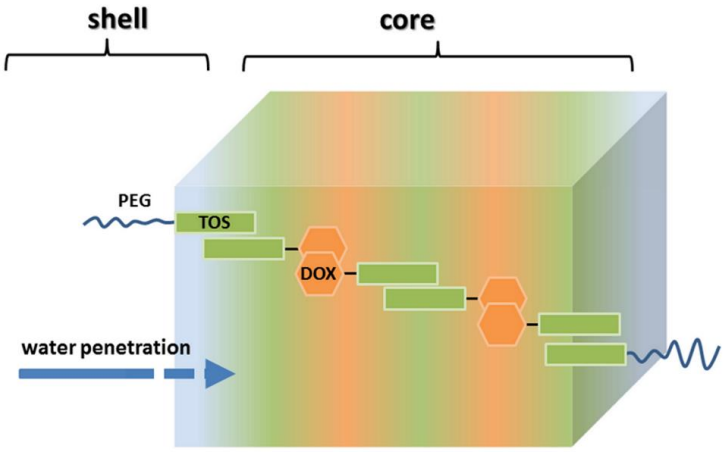

Figure 5. Proposition of N-DOX-TOS nanoparticle structure from the 1H NMR spectrum interpretation.

The release of DOX from the N-DOX-TOS nanoparticles was tested in PBS (pH 7.4) during 1 week at 25°C by using a dialysis method. Results showed that it was not possible to quantify any free DOX within 12h. After 7 days, the amount of DOX released from N-DOX-TOS nanoparticles was less than 2%. (Fig. 6). The stability of the N-DOX-TOS nanoparticles was investigated at 4°C during 6 months. No size changes could be observed in comparison with the initial nanoparticles, supporting high long-term stability (Table 1). This is due to the presence of PEG aqueous layer which provides steric hindrance. Thus, these experiments demonstrate that N-DOX-TOS nanoparticles are stable.

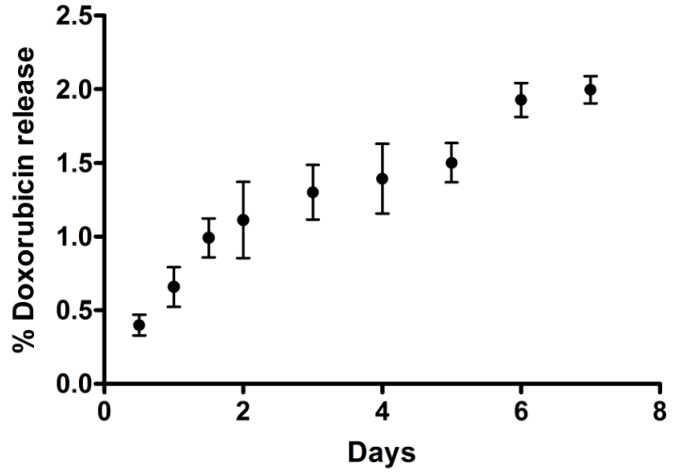

Figure 6. Release of doxorubicin from N-DOX-TOS (N=3).

III.4. CYTOTOXICITY AND CELLULAR UPTAKE OF N-DOX-TOS NANOPARTICLES

The cytotoxicity of N-DOX-TOS nanoparticles was assessed in vitro on the MCF-7 cell line in comparison with free DOX and the physical mixture of DOX, $TPGS_{2000}$ and TOS (DOX+TPGS+TOS), after 24h, 48h and 72h of culture. MCF-7 breast cancer cell line was chosen as model since the effect of DOX have been extensively studied on this cell line (*19, 36, 37*).

The cytotoxicity of N-DOX-TOS nanoparticles, DOX+TPGS+TOS and DOX was time-dependent ($p<0.01$). The IC_{50} of DOX, DOX+TPGS+TOS and N-DOX-TOS are shown in Figure 7 (data in Supporting Information S5). IC50 values of DOX were similar to those previously reported (*19*). The differences between DOX solution, DOX+TPGS+TOS and N-DOX-TOS nanoparticles in inhibiting growth of MCF7 cells was highly significant ($p<0.001$) after 24 h. No significant differencies was observed within three groups after 48 h ($p > 0.05$) and 72 h ($p > 0.05$).

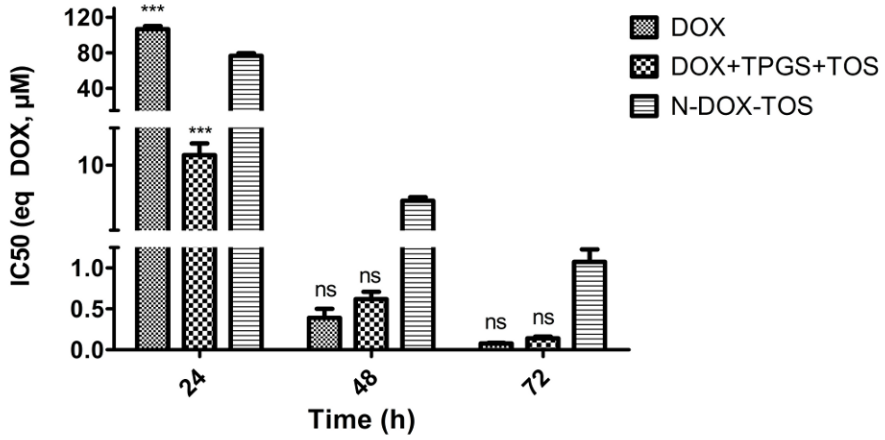

Figure 7. IC50 values of DOX, DOX+TPGS+TOS and N-DOX-TOS nanoparticles in DOX equivalent. Statistical differences are shown using N-DOX-TOS as a benchmark (* = p <0.001, ns means p>0.05, vs N-DOX-TOS; N=3, n=4).**

The prodrug nanoparticles exhibited higher cytotoxicity after 24h in comparison to DOX. This advantage was not shown for longer times of cell incubation. After 48h and 72h, N-DOX-TOS nanoparticles were less toxic than the free drug and the components of the nanoparticles (DOX+TPGS+TOS). The higher toxicity of N-DOX-TOS nanoparticle in comparison to DOX after 24h might be due to the activity of the released vitamin E derivatives. It has been found that TOS and TPGS are able to induce apoptosis and to increase antitumor effect (*18, 38-40*). These data were confirmed on MCF-7 cells as shown in Figure 8 (data in Supporting Information S6). Synergestic effect between DOX and vitamin E derivatives was clearly observed after 24h when cells were incubated with DOX+TPGS+TOS. However this effect was no longer significant after 48h and 72 h. N-DOX-TOS nanoparticles were less effective than DOX+TPGS+TOS after 24h which might indicate an incomplete or delayed conversion to the parent drug. The lower cytotoxicity of N-DOX-TOS nanoparticles after 48h and 72h may be explained for the same reasons. This is a common limitation of hydrophobic prodrugs since their applicability depends on their susceptibility to hydrolytic and/or enzymatic activation. This is consistent with the high stability of amide derivatives as shown in studies on PEG-DOX derivatives (*41*).

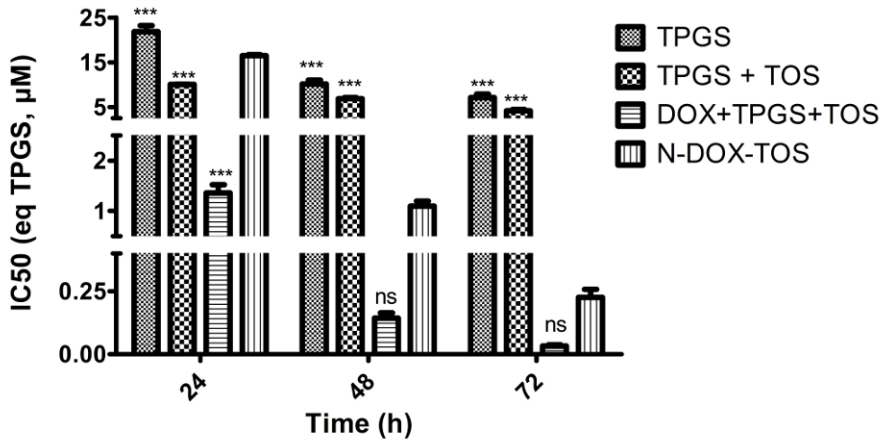

Figure 8. IC50 values of TPGS, TPGS+TOS, DOX+TPGS+TOS and N-DOX-TOS nanoparticles in TPGS equivalent. Statistical differences are shown using N-DOX-TOS as a benchmark (* = p <0.001, ns means p>0.05, vs N-DOX-TOS; N=3, n=4).**

The cellular uptake of DOX and N-DOX-TOS nanoparticles was qualitatively investigated by microscopy after 24h of incubation with MCF-7 cells (Fig 9). The free DOX was totally distributed in the nucleus of the cells since the colors of the DAPI-labeled nucleus (Fig 9 A1) and the DOX (Fig 9 A2) can be perfectly overlayed. N-DOX-TOS nanoparticles were characterized by a broad intracellular distribution with red detection inside and around the nucleus (Fig 9 B1-2). The change in intracellular distribution could play a significant role for the activity of the drug as it was already reported for TPGS-DOX conjugates and PEG-DOX (*19, 41*). The delivery of the prodrug nanoparticles into the cells may occur in a different way from that of the free drug. This may considerably influence the mode of action and the toxicity of the N-DOX-TOS nanoparticles (*41*).

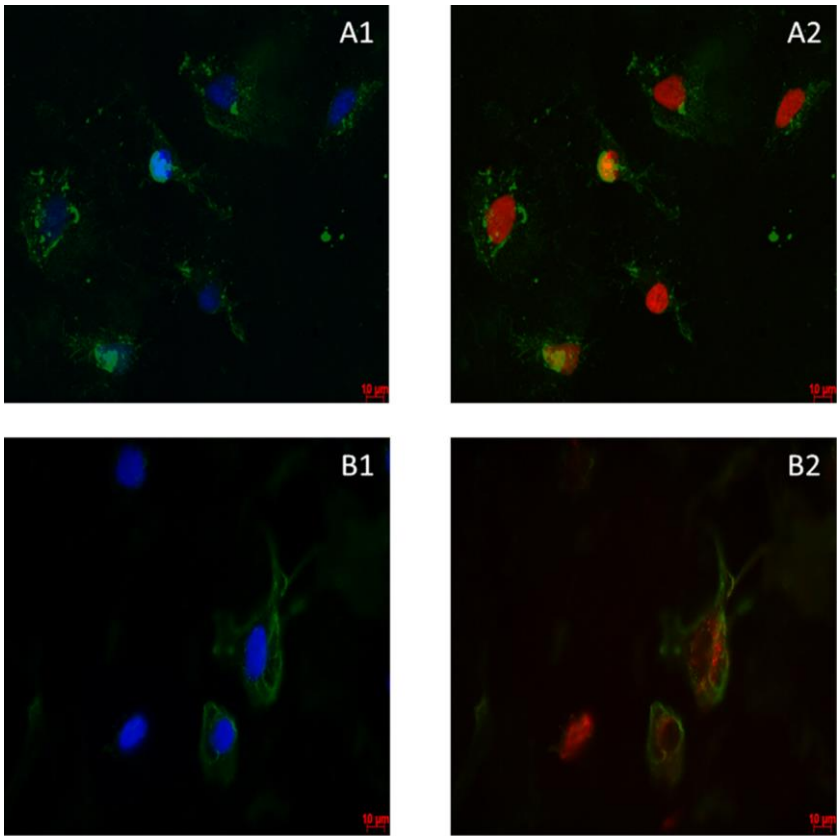

Figure 9. Detection of fluorescent DOX (red) in MCF-7 cells after 24 h incubation with (A) the free DOX and (B) N-DOX-TOS nanoparticles at 10 µM equivalent of DOX. DAPI (blue) and ConA (green) staining were used to label nuclei and membranes, respectively.

IV. CONCLUSION

Our objective was to develop self-assembling prodrug of DOX and vitamin E with a high drug loading to take advantage of the EPR effect of nanoparticulate systems and the biological activity of vitamin E derivatives. The new DOX prodrug self-assemble into nanoparticles showing an internal lamellar microphase separated structure in presence of TPGS as stabilizer. N-DOX-TOS is located in the core of the nanoparticles while PEG chains are in the corona. A high drug loading (34%) and low *in vitro* drug release, compatible with DOX clinical use, were achieved. Significant cytotoxic activity and cellular uptake of N-DOX-TOS nanoparticles were observed. Our design of nanomedicines consisting of N-DOX-TOS and TPGS, could provide a sustained and passively targeted DOX delivery which might reduce DOX toxicity and improve DOX efficacy *in vivo*. Studies are ongoing to further confirm this hypothesis.

V. REFERENCES

(1) Huan, M. L., Zhou, S. Y., Teng, Z. H., Zhang, B. L., Liu, X. Y., Wang, J. P., and Mei, Q. B. (2009) Conjugation with alpha-linolenic acid improves cancer cell uptake and cytotoxicity of doxorubicin. *Bioorganic & medicinal chemistry letters*, *19*, 2579-2584.

(2) Aroui, S., Brahim, S., Waard, M. D., and Kenani, A. (2010) Cytotoxicity, intracellular distribution and uptake of doxorubicin and doxorubicin coupled to cell-penetrating peptides in different cell lines: a comparative study. *Biochemical and biophysical research communications*, *391*, 419-425.

(3) Chhikara, B. S., St Jean, N., Mandal, D., Kumar, A., and Parang, K. (2011) Fatty acyl amide derivatives of doxorubicin: synthesis and in vitro anticancer activities. *European journal of medicinal chemistry*, *46*, 2037-2042.

(4) Talelli, M., Morita, K., Rijcken, C. J., Aben, R. W., Lammers, T., Scheeren, H. W., van Nostrum, C. F., Storm, G., and Hennink, W. E. (2011) Synthesis and characterization of biodegradable and thermosensitive polymeric micelles with covalently bound doxorubicin-glucuronide prodrug via click chemistry. *Bioconjugate chemistry*, *22*, 2519-2530.

(5) Fang, J. Y., and Al-Suwayeh, S. A. (2012) Nanoparticles as delivery carriers for anticancer prodrugs. *Expert opinion on drug delivery*, *9*, 657-669.

(6) Wong, A. D., Dewit, M. A., and Gillies, E. R. (2011) Amplified release through the stimulus triggered degradation of self-immolative oligomers, dendrimers, and linear polymers. *Advanced drug delivery reviews*.

(7) She, W., Luo, K., Zhang, C., Wang, G., Geng, Y., Li, L., He, B., and Gu, Z. (2013) The potential of self-assembled, pH-responsive nanoparticles of mPEGylated peptide dendron-doxorubicin conjugates for cancer therapy. *Biomaterials*, *34*, 1613-1623.

(8) Danhier, F., Feron, O., and Preat, V. (2010) To exploit the tumor microenvironment: Passive and active tumor targeting of nanocarriers for anti-cancer drug delivery. *Journal of controlled release : official journal of the Controlled Release Society*, *148*, 135-146.

(9) Vemula, P. K., Wiradharma, N., Ankrum, J. A., Miranda, O. R., John, G., and Karp, J. M. (2013) Prodrugs as self-assembled hydrogels: a new paradigm for biomaterials. *Current opinion in biotechnology*.

(10) Gong, X., Moghaddam, M. J., Sagnella, S. M., Conn, C. E., Danon, S. J., Waddington, L. J., and Drummond, C. J. (2011) Lyotropic liquid crystalline self-assembly material behavior and nanoparticulate dispersions of a phytanyl pro-drug analogue of capecitabine-a chemotherapy agent. *ACS applied materials & interfaces*, *3*, 1552-1561.

(11) Tang, H., Murphy, C. J., Zhang, B., Shen, Y., Sui, M., Van Kirk, E. A., Feng, X., and Murdoch, W. J. (2010) Amphiphilic curcumin conjugate-forming nanoparticles as anticancer prodrug and drug carriers: in vitro and in vivo effects. *Nanomedicine*, *5*, 855-865.

(12) Bildstein, L., Pili, B., Marsaud, V., Wack, S., Meneau, F., Lepetre-Mouelhi, S., Desmaele, D., Bourgaux, C., Couvreur, P., and Dubernet, C. (2011) Interaction of an amphiphilic squalenoyl prodrug of gemcitabine with cellular membranes. *European journal of pharmaceutics and biopharmaceutics : official journal of Arbeitsgemeinschaft fur Pharmazeutische Verfahrenstechnik e.V*, *79*, 612-620.

(13) Couvreur, P., Reddy, L. H., Mangenot, S., Poupaert, J. H., Desmaele, D., Lepetre-Mouelhi, S., Pili, B., Bourgaux, C., Amenitsch, H., and Ollivon, M. (2008) Discovery of new hexagonal supramolecular nanostructures formed by squalenoylation of an anticancer nucleoside analogue. *Small*, *4*, 247-253.

(14) Reddy, L. H., Ferreira, H., Dubernet, C., Mouelhi, S. L., Desmaele, D., Rousseau, B., and Couvreur, P. (2008) Squalenoyl nanomedicine of gemcitabine is more potent after oral administration in leukemia-bearing rats: study of mechanisms. *Anti-cancer drugs*, *19*, 999-1006.

(15) Prasad, K. N., Kumar, B., Yan, X. D., Hanson, A. J., and Cole, W. C. (2003) Alpha-tocopheryl succinate, the most effective form of vitamin E for adjuvant cancer treatment: a review. *Journal of the American College of Nutrition*, *22*, 108-117.

(16) Kline, K., Yu, W., and Sanders, B. G. (2004) Vitamin E and breast cancer. *The Journal of nutrition*, *134*, 3458S-3462S.

(17) Pussinen, P. J., Lindner, H., Glatter, O., Reicher, H., Kostner, G. M., Wintersperger, A., Malle, E., and Sattler, W. (2000) Lipoprotein-associated alpha-tocopheryl-succinate inhibits cell growth and induces apoptosis in human MCF-7 and HBL-100 breast cancer cells. *Biochimica et biophysica acta*, *1485*, 129-144.

(18) Zhang, X., Peng, X., Yu, W., Hou, S., Zhao, Y., Zhang, Z., Huang, X., and Wu, K. (2011) Alpha-tocopheryl succinate enhances doxorubicin-induced apoptosis in human gastric cancer cells via promotion of doxorubicin influx and suppression of doxorubicin efflux. *Cancer letters*, *307*, 174-181.

(19) Cao, N., and Feng, S. S. (2008) Doxorubicin conjugated to D-alpha-tocopheryl polyethylene glycol 1000 succinate (TPGS): conjugation chemistry, characterization, in vitro and in vivo evaluation. *Biomaterials*, *29*, 3856-3865.

(20) Reddy, L. H., Dubernet, C., Mouelhi, S. L., Marque, P. E., Desmaele, D., and Couvreur, P. (2007) A new nanomedicine of gemcitabine displays enhanced anticancer activity in sensitive and resistant leukemia types. *Journal of controlled release : official journal of the Controlled Release Society*, *124*, 20-27.

(21) Mi, Y., Liu, Y., and Feng, S. S. (2011) Formulation of Docetaxel by folic acid-conjugated d-alpha-tocopheryl polyethylene glycol succinate 2000 (Vitamin E TPGS(2k)) micelles for targeted and synergistic chemotherapy. *Biomaterials*, *32*, 4058-4066.

(22) Steichen, S. D., Caldorera-Moore, M., and Peppas, N. A. (2012) A review of current nanoparticle and targeting moieties for the delivery of cancer therapeutics. *European journal of pharmaceutical sciences : official journal of the European Federation for Pharmaceutical Sciences*, *48*, 416-427.

(23) Arias, J. L., Reddy, L. H., Othman, M., Gillet, B., Desmaele, D., Zouhiri, F., Dosio, F., Gref, R., and Couvreur, P. (2011) Squalene based nanocomposites: a new platform for the design of multifunctional pharmaceutical theragnostics. *ACS nano*, *5*, 1513-1521.

(24) Brigger, I., Dubernet, C., and Couvreur, P. (2002) Nanoparticles in cancer therapy and diagnosis. *Advanced drug delivery reviews*, *54*, 631-651.

(25) Barenholz, Y. (2012) Doxil(R)--the first FDA-approved nano-drug: lessons learned. *Journal of controlled release : official journal of the Controlled Release Society*, *160*, 117-134.

(26) Zhang, Z., Tan, S., and Feng, S. S. (2012) Vitamin E TPGS as a molecular biomaterial for drug delivery. *Biomaterials*, *33*, 4889-4906.

(27) Huober, J., Fett, W., Nusch, A., Neise, M., Schmidt, M., Wischnik, A., Gerhardt, S., Goehler, T., Luck, H. J., and Rost, A. (2010) A multicentric observational trial of pegylated liposomal doxorubicin for metastatic breast cancer. *BMC cancer*, *10*, 2.

(28) Wang, J., Sun, J., Chen, Q., Gao, Y., Li, L., Li, H., Leng, D., Wang, Y., Sun, Y., Jing, Y., Wang, S., and He, Z. (2012) Star-shape copolymer of lysine-linked di-tocopherol polyethylene glycol 2000 succinate for doxorubicin delivery with reversal of multidrug resistance. *Biomaterials*, *33*, 6877-6888.

(29) Yoo, H. S., Lee, K. H., Oh, J. E., and Park, T. G. (2000) In vitro and in vivo anti-tumor activities of nanoparticles based on doxorubicin-PLGA conjugates. *Journal of controlled release : official journal of the Controlled Release Society*, *68*, 419-431.

(30) Park, J., Fong, P. M., Lu, J., Russell, K. S., Booth, C. J., Saltzman, W. M., and Fahmy, T. M. (2009) PEGylated PLGA nanoparticles for the improved delivery of doxorubicin. *Nanomedicine : nanotechnology, biology, and medicine*, *5*, 410-418.

(31) Lei, T., Srinivasan, S., Tang, Y., Manchanda, R., Nagesetti, A., Fernandez-Fernandez, A., and McGoron, A. J. (2011) Comparing cellular uptake and cytotoxicity of targeted drug carriers in

cancer cell lines with different drug resistance mechanisms. *Nanomedicine : nanotechnology, biology, and medicine*, *7*, 324-332.

(32) Spicer, P. T. (2005) Progress in liquid crystalline dispersions: Cubosomes. *Current Opinion in Colloid & Interface Science*, *10*, 274-279.

(33) Israelachvili, J. (1994) The science and applications of emulsions — an overview. *Colloids and Surfaces A: Physicochemical and Engineering aspects*, 1-8.

(34) Caron, J., Maksimenko, A., Wack, S., Lepeltier, E., Bourgaux, C., Morvan, E., Leblanc, K., Couvreur, P., and Desmaele, D. (2013) Improving the Antitumor Activity of Squalenoyl-Paclitaxel Conjugate Nanoassemblies by Manipulating the Linker between Paclitaxel and Squalene. *Advanced healthcare materials*, *2*, 172-185.

(35) Desmaele, D., Gref, R., and Couvreur, P. (2012) Squalenoylation: a generic platform for nanoparticular drug delivery. *Journal of controlled release : official journal of the Controlled Release Society*, *161*, 609-618.

(36) Shieh, M. J., Hsu, C. Y., Huang, L. Y., Chen, H. Y., Huang, F. H., and Lai, P. S. (2011) Reversal of doxorubicin-resistance by multifunctional nanoparticles in MCF-7/ADR cells. *Journal of controlled release : official journal of the Controlled Release Society*, *152*, 418-425.

(37) Tevyashova, A., Sztaricskai, F., Batta, G., Herczegh, P., and Jeney, A. (2004) Formation of squaric acid amides of anthracycline antibiotics. Synthesis and cytotoxic properties. *Bioorganic & medicinal chemistry letters*, *14*, 4783-4789.

(38) Guo, Y., Luo, J., Tan, S., Otieno, B. O., and Zhang, Z. (2013) The applications of Vitamin E TPGS in drug delivery. *European journal of pharmaceutical sciences : official journal of the European Federation for Pharmaceutical Sciences*.

(39) Turanek, J., Wang, X. F., Knotigova, P., Koudelka, S., Dong, L. F., Vrublova, E., Mahdavian, E., Prochazka, L., Sangsura, S., Vacek, A., Salvatore, B. A., and Neuzil, J. (2009) Liposomal formulation of alpha-tocopheryl maleamide: in vitro and in vivo toxicological profile and anticancer effect against spontaneous breast carcinomas in mice. *Toxicology and applied pharmacology*, *237*, 249-257.

(40) Youk, H. J., Lee, E., Choi, M. K., Lee, Y. J., Chung, J. H., Kim, S. H., Lee, C. H., and Lim, S. J. (2005) Enhanced anticancer efficacy of alpha-tocopheryl succinate by conjugation with polyethylene glycol. *Journal of controlled release : official journal of the Controlled Release Society*, *107*, 43-52.

(41) Rodrigues, P. C., Beyer, U., Schumacher, P., Roth, T., Fiebig, H. H., Unger, C., Messori, L., Orioli, P., Paper, D. H., Mulhaupt, R., and Kratz, F. (1999) Acid-sensitive polyethylene glycol conjugates of doxorubicin: preparation, in vitro efficacy and intracellular distribution. *Bioorganic & medicinal chemistry*, *7*, 2517-2524.

VI. SUPPORTING INFORMATION

S1. SYNTHESIS OF N-D-A-TOCOPHEROL SUCCINATE CYTARABINE AMIDE

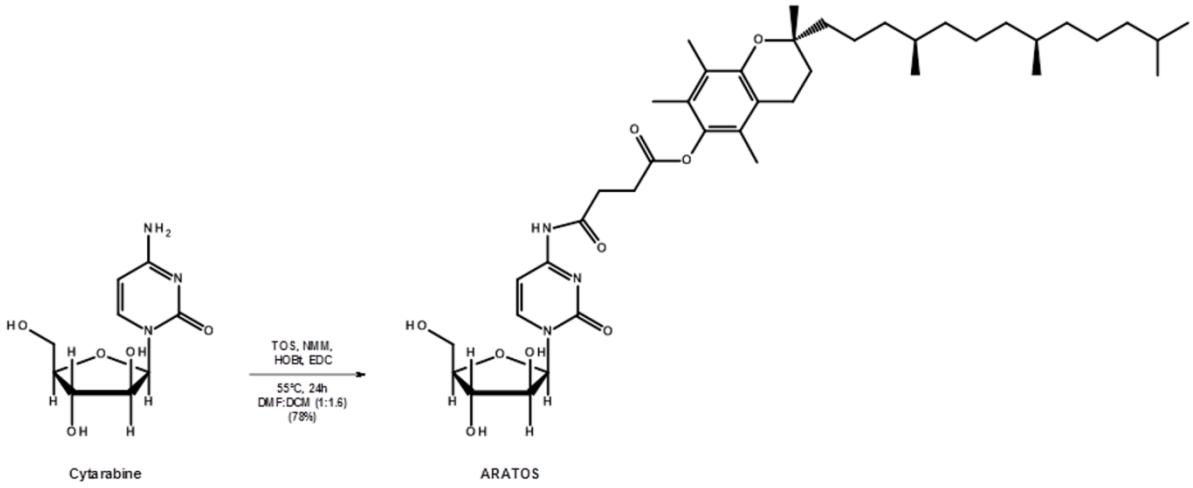

Figure S1. Synthesis of N-D-α-Tocopherol succinate cytarabine amide.

In a 50 mL round bottomed flask equipped with a magnetic stirrer and a cooler, Cytarabine (250 mg, 1.03 mmol) was dissolved in 3 mL of DMF, then was added in the following order N-Methyl Morpholine (104.0 mg, 1.03 mmol, 1 eq), HOBt.monohydrate (184 mg, 1.2 mmol, 1.2 eq), TOS (455 mg, 1.05 mmol, 1 eq) and finally EDC.HCl (263 mg, 1.4 mmol, 1.3 eq). 3 mL of DMF and 10 mL of DCM were used to rinse the vials and added to the solution. The reaction mixture was stirred for 24 hours at 55°C. The mixture was cooled down to 15°C and 20 mL of DCM were added. The organic layer was then washed four times with 60 mL of brine, dried on $MgSO_4$, filtered, evaporated and dried under vacuum for 24h. The resulting yellow powder (m= 508 mg, 78%, HPLC purity ≥ 93%) was collected and used without further purification.

^{1}H NMR (500 MHz, $CDCl_3$): δ 0.78-0.8 (m, 12H), 0.99 (m, 3H), 1.06 (m, 3H), 1.15 (s, 3H), 1.19 (m, 8H), 1.31 (m, 4H), 1.46 (m, 3H), 1.7 (m, 2H), 1.9 (s, 3H), 1.94 (s, 3H), 2 (s, 3H), 2.5 (m, 2H), 2.89-2.73 (m, 4H), 3.73 (m, 1H), 3.81 (m, 1H), 4.02 (m, 1H), 4.14 (m, 1H), 4.31 (m, 1H), 6.1 (m, 1H), 7.37 (d, 1H, J = 7.2 Hz), 8.13 (d, 1H, J = 7.2 Hz).

^{13}C NMR (125 MHz, $CDCl_3$): δ 11.7 (CH3), 12.0 (CH3), 12.8 (CH3), 19.6 (CH3), 19.7 (CH3), 20.5 (CH2), 21.0 (CH2), 22.5 (CH3), 22.6 (CH3), 23.3 (CH3, conformer), 23.9 (CH3, conformer), 24.4 (CH2), 24.7 (CH2), 27.9 (CH), 28.1 (CH2), 31.1 (CH2), 31.5 (CH2), 32.7 (CH), 32.7 (CH), 37.2 (CH2), 37.4 (CH2), 39.3 (CH2), 39.6 (CH2, conformer), 40.5 (CH2, conformer), 61.5 (CH2), 74.9 (CH), 75.1 (C), 76.7 (CH), 85.6 (CH), 88.2 (CH), 96.4 (CH), 117.4 (CH), 122.9 (C), 124.9 (C), 126.6 (C), 140.4 (C), 146.4 (CH), 149.3 (C), 156.4 (C), 162.3 (CO), 171.7 (CO), 172.2 (CO).

HRMS-ESI (m/z): calculated for C42H66O9N3: [M+H]+ 756,47936, found : 756,47941

λ_{max} (7.10^{-5}M, $CHCl_3$): 244 nm (ε_{max}= 20333), 289 (12273), 300 (11833).

S2. SOLUTION OF NANOPARTICLES OF N-DOX-TOS/TPGS IN WATER AFTER EVAPORATION OF ACETONE.

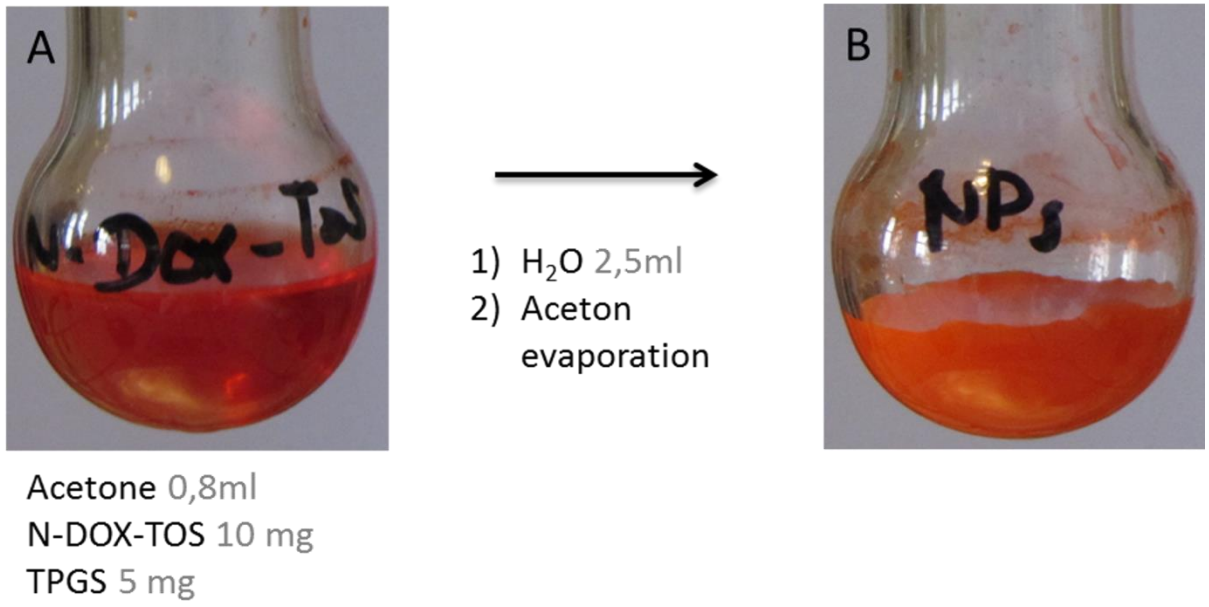

Figure S3. A) Solution of N-DOX-TOS, TPGS in acetone, B) Solution of nanoparticles of N-DOX-TOS/TPGS in water after evaporation of acetone.

S3. INTERPRETATION OF NMR SPECTRA OF N-DOX-TOS NANOPARTICLES

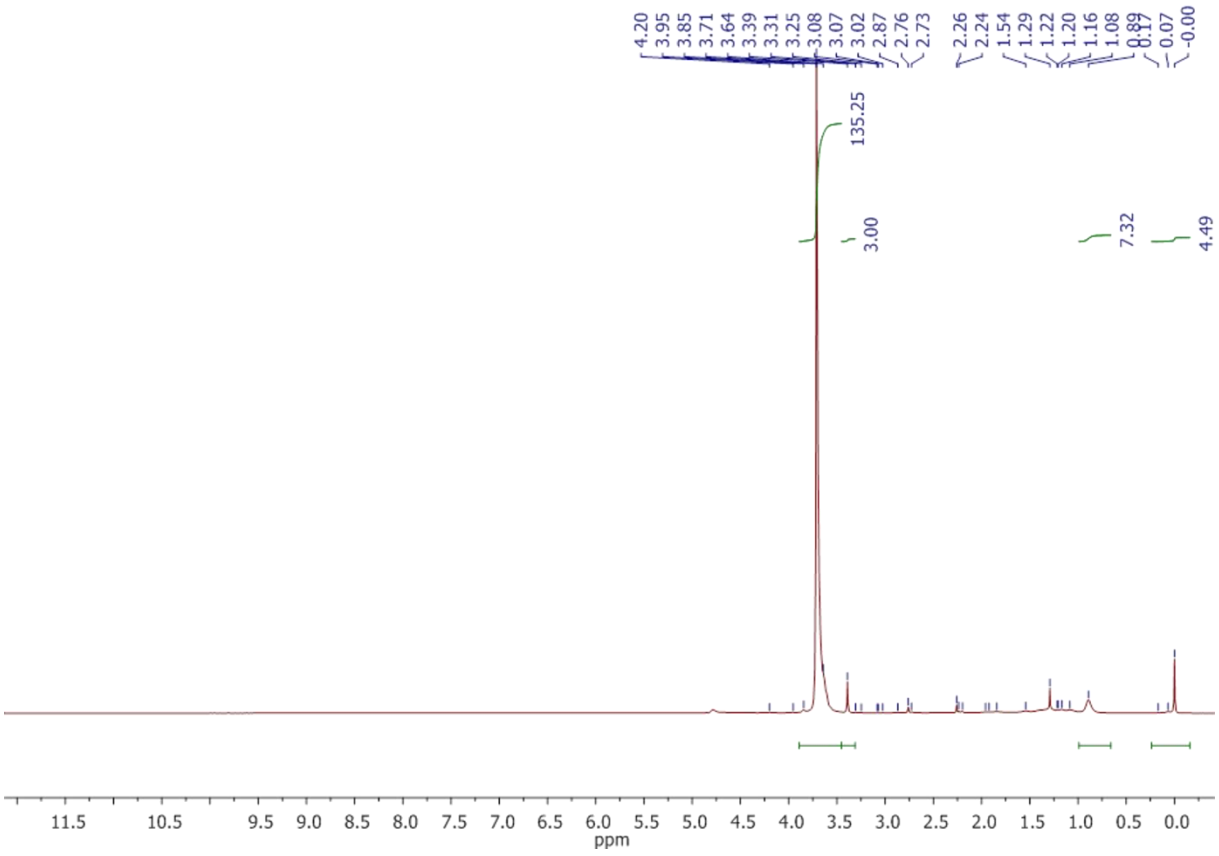

Figure S2. ^{1}H NMR full spectrum in D_2O, with pres-aturation of H_2O protons and with integrations of interesting peaks for the N-DOX-TOS nanoparticles containing N-DOX-TOS and TPGS.

S4. INTEGRAL THEORETICAL CALCULATION FOR THE DETERMINATION OF TOS IN THE NANOPARTICLES AND IN TGPS

$$\frac{Int\ CH_2O - PEG}{Int\ CH_3 - TOS}\ Total = \frac{n_{TPGS} \times n_H \times \left(Mn_{PEG}\ /MM_{CH_2CH_2O}\right)}{\left(n_{TPGS} \times n_H + n_{DOX-TOS} \times n_H\right)} \quad (1)$$

$$\frac{Int\ CH_2O - PEG}{Int\ CH_3 - TOS}\ TPGS = \frac{n_{TPGS} \times n_H \times \left(Mn_{PEG}\ /MM_{CH_2CH_2O}\right)}{\left(n_{TPGS} \times n_H\right)} \quad (2)$$

Equation (1) is for the calculation of the total content of TOS in the nanoparticles; Equation (2) is for the calculation of the contribution of the TOS in TPGS alone; n_{TPGS}, $n_{DOX\text{-}TOS}$ are the amounts in mol of TPGS and DOX-TOS, respectively, n_H is the number of hydrogen for the function or motif considered (*i.e.* 3Hx4 = 12H for the aliphatic CH_3 of TOS and 4H for the PEG repeating unit), Mn_{PEG} is the molecular weight of PEG (2000 g.mol^{-1}), $MM_{CH2CH2O}$ is the molecular weight of PEG repeating unit (44 g.mol^{-1}).

S5. IC50 VALUES OF DOX, N-DOX-TOS NANOPARTICLES AND DOX+TPGS+TOS IN EQUIVALENT μM DOX

Tabe S1. IC50 values (in equivalent μm DOX) of MCF-7 cells incubated with DOX-TOS nanoparticles versus DOX versus DOX+TPGS+TOS for 24, 48, 72 h (N=3, n=4).

	24h	48h	72h
DOX	107 ± 6	0.4 ± 0.2	0.08 ± 0.02
DOX + TPGS + TOS	9 ± 2	0.6 ± 0.2	0.14 ± 0.04
N-DOX-TOS	78 ± 3	5.2 ± 0.8	1.1 ± 0.3

S6. IC50 VALUES OF TPGS, TPGS+TOS, N-DOX-TOS NANOPARTICLES AND DOX+ TPGS+TOS IN EQ μM TPGS

Table S2. IC50 values (in equivalent μM TPGS) of MCF-7 cells incubated with TPGS versus TPGS+TOS versus DOX + TPGS + TOS for 24, 48, 72 h (N=3, n=4).

	24h	48h	72h
TPGS	22 ± 2	10 ± 1	7 ± 1
TPGS + TOS	10.1 ± 0.8	6.8 ± 0.4	4.1 ± 0.4
TPGS + TOS + DOX	1.4 ± 0.4	0.14 ± 0.04	0.033 ± 0.009
N-DOX-TOS	16.4 ± 0.5	1.1 ± 0.2	0.23 ± 0.06